CHALMERS
UNIVERSITY OF TECHNOLOGY

A Physics-Informed Cold-Start Capability for xEV Charging Recommender System

Citation for the original published paper (version of record):
Orbay, R., Singh, A., Emilsson, J. et al (2024). A Physics-Informed Cold-Start Capability for xEV Charging Recommender System. IEEE Open Journal of Vehicular Technology, 5: 1457-1469. http://dx.doi.org/10.1109/OJVT.2024.3469577

(article starts on next page)

IEEE Open Journal of Vehicular Technology

Received 11 September 2024; accepted 17 September 2024. Date of publication 27 September 2024;
date of current version 18 October 2024. The review of this article was coordinated by Editor Yunhong Che.

Digital Object Identifier 10.1109/OJVT.2024.3469577

A Physics-Informed Cold-Start Capability for xEV Charging Recommender System

RAIK ORBAY [1,2], ADITYA PRATAP SINGH [1], JOHANNES EMILSSON[1], MICHELE BECCIANI [3], EVELINA WIKNER [2] (Member, IEEE), VICTOR GUSTAFSON[1], AND TORBJÖRN THIRINGER [1,2] (Senior Member, IEEE)

[1]Volvo Car Corporation - 97100 Propulsion and Energy - Strategy and Execution, Torslanda PVOSG 22, SE-405 31 Gothenburg, Sweden
[2]Department of Electrical Engineering, Chalmers Technology University, SE-412 96 Gothenburg, Sweden
[3]AB Volvo, SE-405 08 Gothenburg, Sweden

CORRESPONDING AUTHOR: RAIK ORBAY (e-mail: raik.orbay@volvocars.com).

ABSTRACT An effortless charging experience will boost electric vehicle (xEV) adoption and assure driver satisfaction. Tailoring the charging experience incorporating smart algorithms introduces an exciting set of development opportunities. The goal of a smart charging algorithm is to lay down an accurate estimation of charging power needs for each user. As recommender systems (RS) are frequently used for tailored services and products, a novel RS based approach is developed in this study. Based on a collaborative-filtering principle, an RS agent will customize charging power transient prioritizing the physical principles governing the battery system, correlated to customer preferences. However, parallel to other RS applications, a collaborative-filtering for charging power transient design may suffer from the cold-start problem. This paper thus aims to prescribe a remedy for the cold-start problem encountered in RS specifically for charging power transient design. The RS is cold-started based on multiphysical modelling, combined with customer driving styles. It is shown that using 7 fundamental charging power transients would capture about 70% of a set of representative charging power transient population. Matching a unsupervised learning based clustering pipeline for 7 possible customer driving styles, an RS agent can prescribe 7 charging power transients automatically and cold-start the RS until more data is available.

INDEX TERMS Electric vehicles, fast charging, heat transfer, physics-aware recommender system, RS cold-start, thermomechatronic modelling.

I. INTRODUCTION

Conforming with the United Nations Sustainable Development goals [1], electrification supports sustainable transportation. However, as the xEVs need to be replenished with frequent intervals, improved charging strategies and availability are crucial for customer satisfaction. The charging experience of the xEV user is shaped by several factors such as xEV configuration, grid and electricity infrastructure, economics, energy and greenhouse gas emissions (GHG) as well as user preferences. The building blocks of the representative ecosystem is shown in Fig. 1, which musters many sub-systems and a vast parameter space. Nowadays large amounts of online and offline data populated in the car, electric vehicle interface (EVI) and various cloud databases enable an accurate prediction base for customer sentiments on the charging experience. As recommender systems (RS) are frequently used for tailored services and products, xEV charging is appropriate as an RS governed smart service.

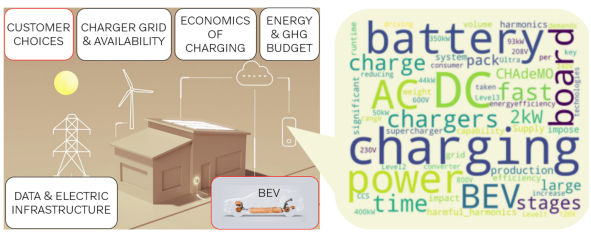

FIGURE 1. Illustration of the charging ecosystem. The two elements in red frames, customer and the xEV sub-systems, are considered in this study. In the inset, various charging terms from recent literature are listed as a word cloud.

A smart fast charging algorithm, thus, can include all the above-described engineering considerations correlated with user preferences. As many customers are actively using social media, car culture portals, consumer sites, and internet forums to share experiences [2], the resulting Big Data has the prospects to determine even the charging experience. On the premises that the charging preferences of the customer will be recognizable patterns in a Big Data repository based on the actual experience with the xEV, an RS can quantify this information to allocate resources for future charging needs. In the herewith proposed smart fast charging scenario, charging power transients tailored for each customer can be prescribed based on the usage data but also the Big Data populated elsewhere as in the Fig. 1.

II. STATEMENT OF THE PROBLEM

The appropriate engineering design of the Big Data supported charging ecosystem is a multi-disciplinary undertake and consists of numerous key-performance indices per multitude of sub-systems. The charging power transient has the purpose of enabling the customer to charge the xEV with maximum amount of energy depending on the available time from the customer's side; but is also restricted by the cost of energy, time of the day, infrastructure capabilities, charger type, traffic situation, weather condition, geographical information, customer preferences, emission restraints, age and state of health (SOH) of the battery and its chemistry, thermal restraints, vehicle design, peak shaving / scheduling, V2X (Vehicle to Everything) needs, etc.

A. CHALLENGES OF FAST CHARGING

Fast charging is controlled by balancing the current from the EVI with the battery pack's charging time, energy loss, and charging constraints [3] or via real-time dynamic queuing [4] as well as power delivery schemes prescribed using EVI hardware [5]. The direct current (DC) on-board fast chargers are typically rated at 50 kW up to 350 kW [6]. Having such high charging power has implications on the SOH of the battery [7]. Repeated heat loads can also weaken structural elements of a battery [8]. Thermal conditioning prior to the fast-charging event is investigated by many authors, as cold temperatures can also undermine battery health [9]. For this reason, earlier work in the available literature devised efficient ways to dissipate efficiently thermal loads due to the losses [10], [11]. Being a multidisciplinary balancing act, the fast-charging power transient waveform has an implication in discipline electromagnetic compatibility (EMC) in power dense xEV architectures. Earlier work from 2016 reports on susceptibility of integrated circuits of battery management system (BMS) could be a major threat to the safety of emerging EVs [12].

From several charging algorithms, the constant-current constant-voltage (CC-CV) charging is the most commonly used charging approach [13] for the Li-ion batteries. In this study, the charging power transients not only include CC-CV mode, but also various other reported charging methods including pulsed waveforms [14], [15].

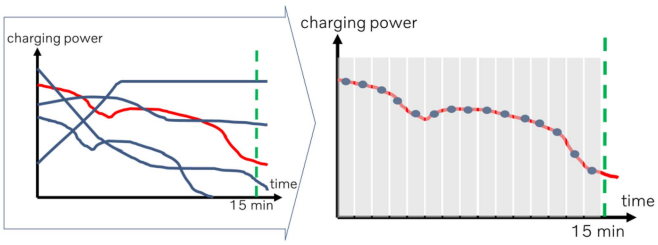

FIGURE 2. B-spline based trial function approach taken to discretize arbitrary charging power transients. 15 minutes are represented as 15 control points per B-spline.

B. COLLOBORATIVE-FILTERING AS AN RS

The collaborative-filtering based RS found widespread adoption for tailored services and consumer products. However, the bulk of the RS research target shopping, music & movies, travel, restaurants, people, and articles [2], [16]. Only a sub-set of the research reported is RS for xEV operation. Zeinab et al. reported on an RS for charging station choice [17], Tan et al. prescribe an RS for BEV taxi charging locations [18]. Wang et al. present findings on BEV wireless charging data security aspects of the recommendations [19]. In a review paper, Teng et al. lists approaches for EV charging demand management [20], which does not report any RS for the charging transient customization purpose. In the proposed approach, trial functions for power transients are created as shown in Fig. 2.

There is a significant knowledge gap in RS applications for smart charging. An approach like the one proposed in this study completely lacks from a recent comprehensive review, where smart systems take the user as a rational agent and focus instead on balancing the grid ability with the demand [21].

It is reported in the literature that a collaborative-filtering based RS will suffer from the cold-start problem in case sufficient data from other customers is lacking [22]. Cold-start issue happens when a RS is deployed but not yet access to sufficient data to draw conclusions about users. In a fast charging scenario, this is the instant when a new customer is receiving their vehicle, or an RS deployed for car sharing purposes does not yet build up a decision base about new drivers. Alternatively, when rental vehicles are rented by new drivers instead of usual corporate customers, there is not yet a large database about the charging habits and xEV usage behavior. Despite the cold-start drawback, RS based systems dominate on-demand services and thus applicable for a on demand fast charging service aiming at automotive industry.

Adding a dimension of customer sentiments, RS can improve the overall charging experience using machine learning (ML). The novelty of the current study is in prescription of a mathematical basis for the RS to operate on. Practically, such an RS for xEV charging would focus on the transfer of the energy into the battery as a power transient as the delivery goal.

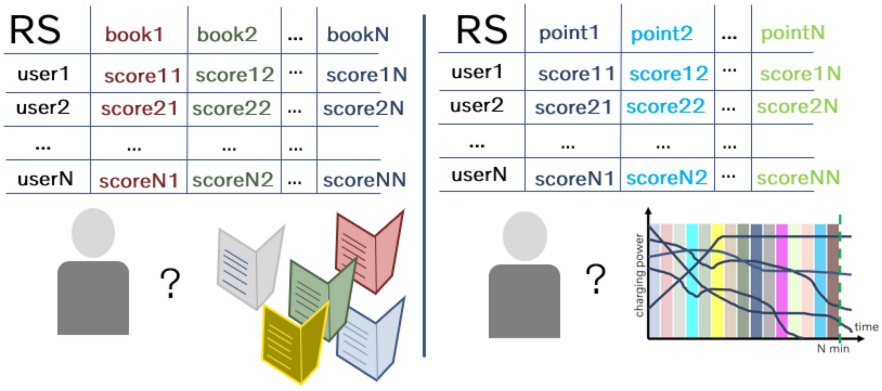

FIGURE 3. The essential for the proposed RS is parallel to collaborative filtering. In the left inset, an RS agent aims to propose a book for a user. In the right inset, another RS agent builds up specific fast charging power transient for a driver.

C. PRESCRIPTION OF A FAST CHARGING RS

Starting from general collaborative-filtering principles, the RS-agents build up products and services to satisfy the customer needs. As shown in Fig. 3 in the left-side inset, an RS for books mathematically establishes a probability density for the customer on liking a new book, based on the former book choices they have enjoyed. The RS for the smart xEV charging will execute a similar mathematical operation, but instead for a charging power transient targeting maximum xEV user satisfaction. To prescribe the charging power transient as a product, the RS agent will use available data to construct charging power transients as mathematical entities. Given that the B-spline based trial function approximation is a surface or curve construction technique which is widely reported in the literature [23], the charging power transients can be deterministically constructed using B-splines.

A B-spline for charging power transient is constructed as a power function in the time domain of an arbitrary duration. Essentially, each control point, aka. knot, on these B-spline forms is a voting instant, as shown in Fig. 3 right-side inset. The voting in this context is an automatized process based on probability densities accumulated by each control point following each charging event by the xEV users. The charging power transients will be quantified after each charging instance, the more a charging power transient control point gets voting from a certain type of xEV user, the more likely that another user in same customer cluster with likely xEV receive a similarly positioned charging curve B-spline control point. In case charging data from earlier customers is not readily available, other usage characteristics which can be correlated to charging can be detected in energy usage, speed distribution, acceleration distribution, rate of road gradients, etc.; an example of this approach is provided in Section VI-F. The probability density gathered from earlier charging events by the xEV customers including their SOC evolution, if available, destination etc. will guide the RS-agent to propose new control point possitions on the power-time surface; this time tailored for the specific xEV user.

For the current study, the inbuilt flexibility of the scripted pipeline allows for an arbitrary duration for the charging events. To align with the contemporary xEV capabilities, the overall charging time for this study is fixed at 15min.

III. AI FRAMEWORK TO PRESCRIBE REALISTIC FAST CHARGING POWER TRANSIENTS

Fast charging data from human users has not been available for this project. Many public data repositories do not provide the actual usage behavior, but rather concentrate on controlled charging-discharging events [24], [25], [26], [27]. To include charging behaviors realistically, charging transients from open literature are studied [28]. However, real charging power transients have not been available for the current project, instead an artificial intelligence (AI) based set up is undertaken to populate a substantial amount of charging power transients acting in battery operating envelope boundaries. Mimicking human users, the AI tasked with populating charging power transient curves also aimed to transfer as much energy into battery as possible. From the AI toolbox, a multi-objective genetic algorithm (MOGA) based optimization pipeline is scripted using Python as depicted in Fig. 4. In the AI governed process, the MOGA agent spawns possible charging power transients evolutionarily for a given fast charging duration. This is realized by improvements on an initially random charging power transient while the MOGA agent explores the overall design parameter space.

As a fail-safe policy, the charging power transients which lead to off-design behavior like high temperatures, mechanical loads, induced electric field rates were discarded. To accurately quantify the operation envelope for the battery, adequate spatial and temporal resolution is required. The detailed multi-physics Finite Element Model (FEM) of a battery pack during fast charging event aims to describe, then tailor using available parameters like thermal conditioning, what a battery can safely deliver to an xEV user. This leads to feasibility of any charging power transient inside the locus of safe vehicle operation and allowed by the EVI.

A battery pack design is chosen to represent the state-of-the-art applications in light duty vehicles. Simplifications are made to include only the key components and properties for fast charging; heat generation from the battery

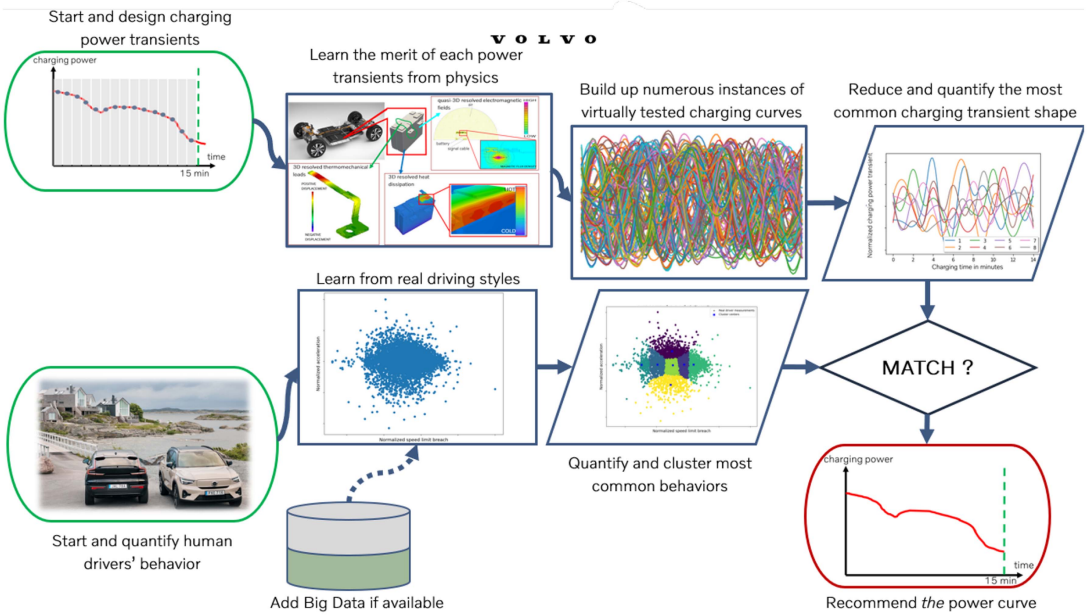

FIGURE 4. **The complete virtual modelling flowchart comprising 0D battery model, 3D thermal, 3D mechanical, quasi-3D electromagnetic and optimization modules.**

cell to the tab, the mechanical stress due to the heat generated on the busbars and the electromagnetic interference (EMI) from switches in the power electronics package, were prioritized. The hierarchical approach starts from system-of systems level. At this level, a Thévenin-circuit based equivalent circuit model for the battery is used to compute generated losses in the fast charging process including instantaneous battery heating and cooling needs. These losses are subsequently passed to a 3D conjugate heat transfer model (CHT) to resolve accurate distribution of hot spots in the chosen battery packaging geometry. Quantified temperature distribution information is likewise fed into structural mechanics computations to pinpoint mechanical loads on soldered battery parts. An additional computation is done to consider the packaging constraints due to EMI.

The MOGA agent discards optimization results which trespass thermal, mechanical or electrical limits of the battery system using specific look-up tables, thus multiobjectively optimized charging power curves are populated. From left to right, two start points in the flowchart on Fig. 4 is discernable. The upper-hand start station is related to automatic creation of charging power transients and their FEM characterization. The lower-hand start station corresponds to real human data, here only the drivestyles are investigated to detect clusters, but method is designed with the flexibility to include more data as shown in Fig. 5.

Data gathered during driving and charging, comprising related social media feeds and similar content with sentiment updates, can all be agglomerated in a big database. Therefore, the lower-hand positioned database station in Fig. 4 is a modular allocation for Big Data, when available once the RS is cold-started. Two fundamental flow structures in the chart on Fig. 4 are met in a matching process. In its simplest from, if

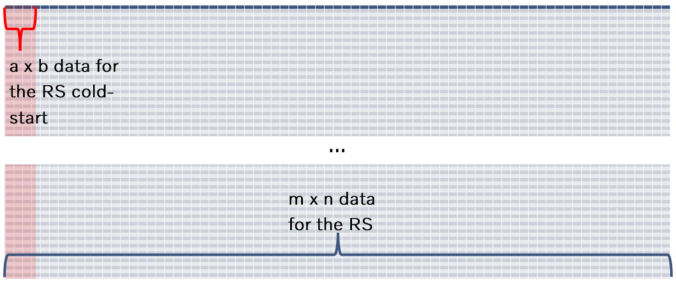

FIGURE 5. **RS feature space. The large dataset including all the customer data; only a subset of this is comprised by the power transient choice done by the customer while EV charging event.**

the number of clusters detected in human driver behavior will be same as principal components contained in innumerable charging power transients populated inside the operating domain of the battery, power transients can be recommended for the actual drivers. This is the result out of the pipeline, which can be based on integral of fast charging power transients, i.e., energy supply with the clustered regions in the driving style plot, which corresponds to energy demand.

Being part of a larger ecosystem of xEV-related RS comprising Big Data, a sub-system for tailored fast charging can be created concentrating solely on the charging power transient as shown in Fig. 5. For the scope and to protect Intellectual Property, further simplifications need to be made. To eliminate the need to resort to various charging characteristics from the drivers, just two features; namely, speed and acceleration data, are used to quantify the driving styles. As hyperplanes of higher orders are impossible to plot, the choice of just two features from the numerous features logged as driver data, enables interpretable plots like in Fig. 6. In this plot normalized speeds per each of the 8 drivers as well as

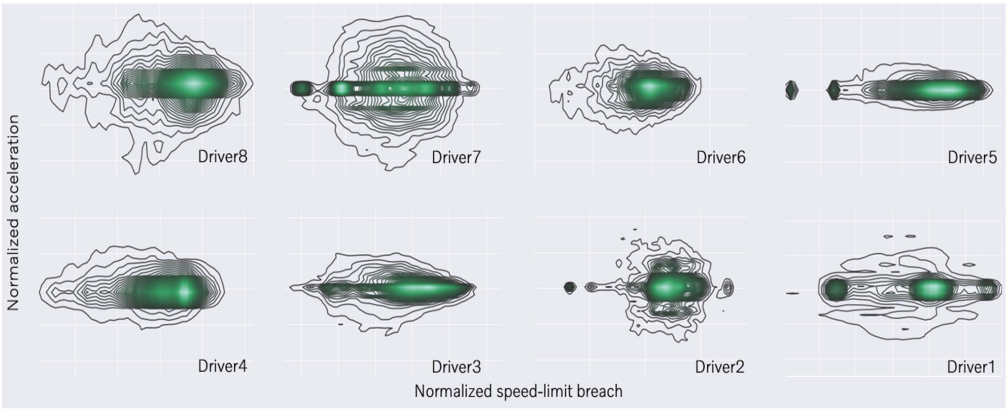

FIGURE 6. Detail of the set of eight individual drivers' acceleration and speed-breach KDE plots. Plots are for same drivers as in the composite image in Fig. 7.

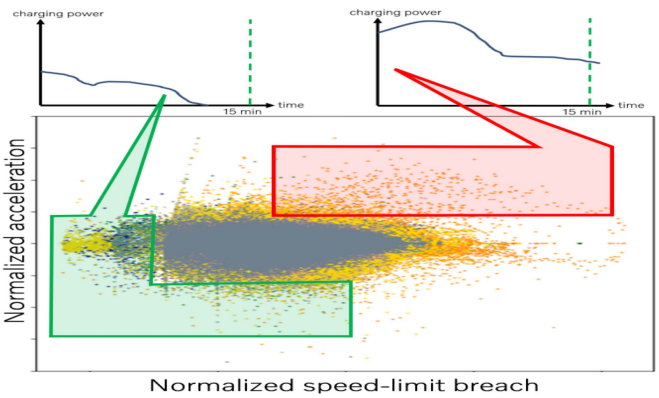

FIGURE 7. Driving dynamics assumed as a cursor for charging needs. For a small set of eight drivers, the user on the left side of the acceleration-speed-limit-breach plot will use less energy, thus, needs less charging power for a comparable trajectory.

speed limit breaches are plotted, where the speed limit breach is the difference between the speed limit at the anonymized GPS position and the actual vehicle speed. A Kernel Density Estimate (KDE) for each of the drivers are investigated for the exploratory analysis [29]. KDEs for bivariate functions transform the data using continuous probability density distributions. These plots show the diverse driving habits among the drivers, e.g., Driver8 consumes more energy than the Driver1, thus will need more charging instances for a given trajectory. Accordingly, it is assumed that the drivers with higher speeds and accelerations are the ones which will need more energy content in their power transients. For drivers who are placid, the situation will be the vice-versa as depicted in Fig. 7. Many methods from ML are available to discern and classify driving styles, which may lead to detection of the energy consumption, vehicle dynamics, aggressivity, usage patterns, etc. Appropriately, a K-means based clustering is used to find patterns in driving habits of drivers [30]. As shown in Fig. 8 for eight drivers, unsupervised clustering approaches are able to cluster the dataset in same number of clusters, albeit in different morphologies.

To match the user preferences in fast charging, the FEM based charging power transient set further used to create reduced order charging power transients using a pattern recognition algorithm from the ML toolbox. While discerning the most important charging power transients, order reduction process keeps the most relevant features, which relates to the most dominant charging power transient waveforms, used by the assumed xEV users. This is achieved using unsupervised learning where a Principal Component Analysis (PCA) of the charging power transients removes charging power transients of least usage, as this set of power transients would correspond to the set of xEV users at the fringes of the fast charging behavior. To combine the battery behavior with customer choice prediction, real driving data of eight customers is investigated. It is assumed that the driving style of the drivers will be a cursor for their energy usage, thus their charging needs.

In the case of modeling for battery modules and packs, the heat generation and heat transfer between the connectors differ due to manufacturing which also leads to an inconsistency between cells within the pack. The AI pipeline allows for extra robustness search by creating additional candidates with geometry morph. A Python script-based module which changes CAD prior to meshing is prepared but not used for the reported work.

IV. EXPERIMENTAL DATA

To relate the possible charging power transients to the human drivers, anonymized data from 50 drivers is used [31]. Comprising only 50 drivers, the dataset used for this study is relatively limited. However, this is aligned with a RS cold-start scenario, where there is scarce data on the charging traits of the customer. Additionally, there also is a general trend towards smaller datasets, for instance insufficient dataset usage in health [32], small datasets for transformers [33], small datasets <5000 samples in software engineering [34] are recently reported. The research on small datasets are mostly investigated for image processing [35], thus, the current study tackles another domain for small dataset application.

The total number of AI populated power transients are only limited by the available High Performance Computing (HPC) resources, thus in theory, an infinite set of variants of charging power transients are possible to capture all the smart charging design space.

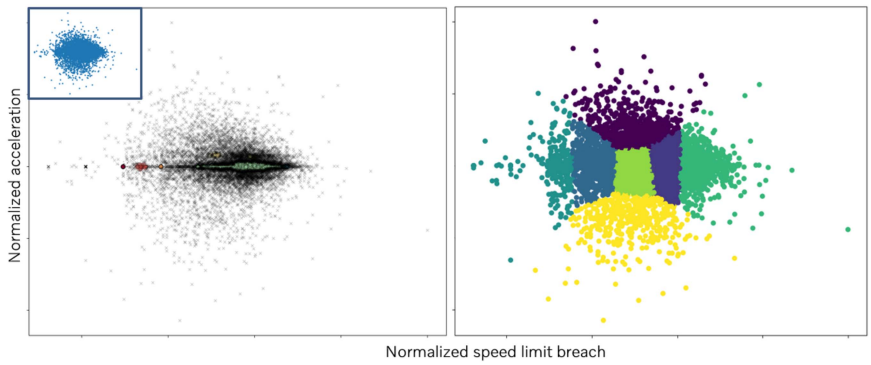

FIGURE 8. Clustering of drivestyles for eight drivers. HDBSCAN clustering on the lefthand image and K-means clustering on the righthand side image. In the small inset, the original distribution shown in blue point scatter.

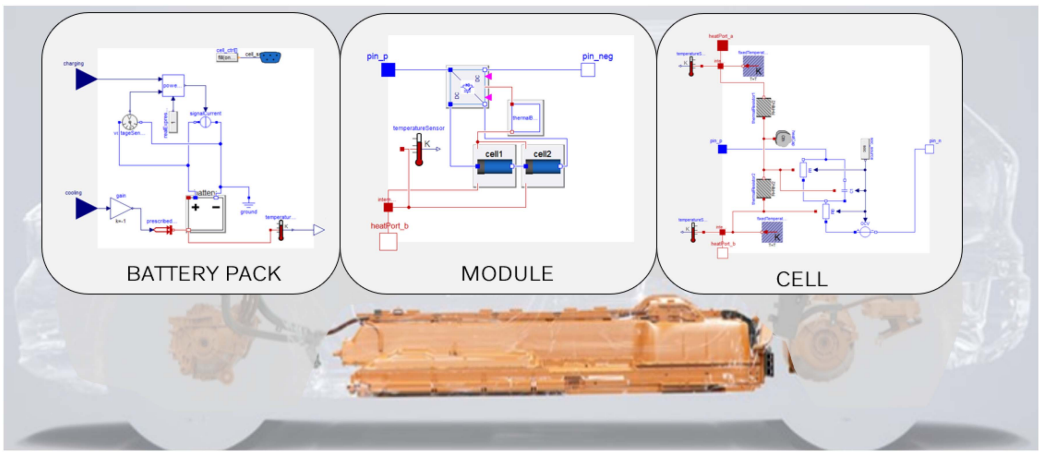

FIGURE 9. Vehicle as a system-of-systems level modelling instance. The battery in orange in the figure is cascaded into its modules and cells.

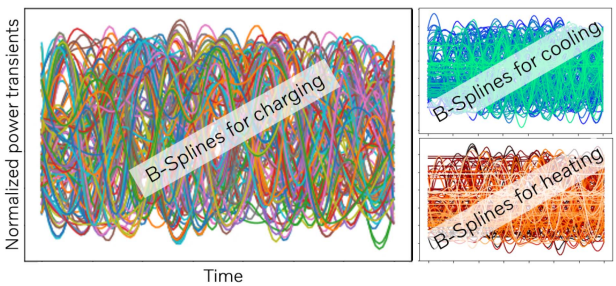

FIGURE 10. Illustration of innumerable charging transients captured by AI. Three set of transients are of interest: charging power transient, cooling and heating power transients.

V. COMPUTATIONAL APPROACH

In this work charging events are modelled as power transients provided by the EVI to the vehicle On-Board Charging (OBC) unit, which are simulated using FEM. As the battery chemistry thrives at certain ambient temperatures, the thermal conditioning of each cell is even more crucial for fast charging [11]. To better capture the physics, the power transients for heating and cooling of the battery are also computed. As illustrated in Fig. 10, thermal effects on charging are modeled by individual power transients designed by AI. When all the reasonable charging transients are created based on detailed physics, it will allow for further studies in pattern recognition as will be described in Section V-F. Only when thermal conditioning is included, the setup will enable the system to be connected to customer choices and preferences. In this way a thermomechatronically dimensioned charging transient will be prescribed for the customer.

A. SYSTEM-OF-SYSTEMS LEVEL MODELLING

A MOGA based approach is chosen for system-of-systems level quantification. In MOGA, the individuals with the best gene pool will survive the natural selection, transmitting their DNA for later generations. This will be reflected on the choice of concept solutions from the concept pool populated using FEM in several disciplines. Analogue to four biological processes in nature; reproduction, mutation, recombination, and selection, the MOGA will deem the merit of each concept solution per investigated discipline. The mathematical model of this theory starts with a randomly selected population of concept designs on the parameter space, where each of the unique design parameters form a DNA [36]. Through an iterative process, the algorithm reaches to a design point in the solution domain that minimizes the objectives of the optimization. An in-built randomness in this process enables the algorithm to perform well in several optimization problems

encountered in automotive system design, as the algorithm is agnostic about the gene pool. Subsequently, the MOGA agent creates a pool of generations, monitoring the concept designs on the parameter space by evaluating their fitness. The algorithm then selects the parents for the next generations from the set of fittest concept designs. The crossover and mutation operations are then used to create new offsprings in the concept design domain. Finally, the algorithm discards the least fit concept solutions to ensure survival of the fittest.

For the reported research, the MOGA is tuned for problems involving discrete variables and an evolution strategy with self-adaptation for problems with continuous variables is incorporated [36]. For this, the AI software makes use of a two-point crossover technique to exchange genetic string values between the members of the population during the EA breeding process. A cross-over rate of 0.8 is chosen.

B. SYSTEMS LEVEL MODELLING

A complete High Voltage (HV) system of a representative xEV is modeled using Modelica language [37]. The schematics of various levels of system modelling is shown in the lower part of the Fig. 9 where the detail is cascading from battery level on the left-hand side subplot, to module level in the middle subplot, and finally to cell level in the right hand side subplot. As the AI based approach needs to populate an extensive number of charging power transients to learn from, the speed of the system-of-systems level model is of crucial importance. A surrogate model is prepared for this purpose. To present battery, module, and cell system models, a Functional Mock-up Interface (FMI) is prescribed. The MOGA agent uses the FMI comprising of a battery pack and its charging as well as the thermal conditioning input for the optimizing the cooling power transient as illustrated in the Fig. 10. The MOGA is used to reduce the battery losses and to come up with the dynamic charging and cooling power transients within the dedicated charging time. The FMI also comprises of the thermal path consisting of bus bar, dielectric thermal conductor sheet and aluminum sheet to the car body. The thermal conditions governed by a time dependent energy equation modified from [38] as shown in (1).

$$mC_P\left(\frac{dT}{dt}\right) = I\left(U_{OCV} - V\right) + IT\left(\frac{\partial U_{OCV}}{\partial T}\right) + hA\left(T - T_{amb}\right) + P_{cool/heat} \tag{1}$$

In (1), C_P is the specific heat of each material at constant pressure and h is the convective heat transfer coefficient. I represents the current through the tabs of the battery. V is the battery voltage. T is the battery temperature under the actual boundary conditions and T_{amb} is the temperature field experienced by the battery. $P_{cool/heat}$ is the term representing the power expended for cooling or heating the battery as needed. U_{OCV} is the open circuit (or equilibrium) voltage [39].

C. DISCIPLINE HEAT TRANSFER

In the Finite Volume Method, Navier-Stokes equations and the energy equation for fluids and solids are discretized over elements constituting a computational mesh representation of the battery module [40]. The solver used is chtMultiRegionSimpleFoam from the OpenFOAM CFD tool [41]. As described in the source code header, chtMultiRegionSimpleFoam is a steady solver for buoyant, turbulent fluid flow and solid heat conduction with conjugate heat transfer between solid and fluid regions [41]. The solver handles the fluid domain continuity as

$$\frac{\partial \rho}{\partial t} + \nabla \cdot (\rho \boldsymbol{u}) = 0 \tag{2}$$

where $\boldsymbol{u}$ is the velocity vector and ρ is the fluid density.

Subsequently, the momentum in the fluid domain is modelled by the Navier-Stokes equation in 3D as

$$\frac{\partial (\rho \boldsymbol{u})}{\partial t} + \nabla \cdot (\rho \boldsymbol{u}\boldsymbol{u}) + \nabla \cdot (\mu \nabla \boldsymbol{u}) \nabla \cdot \left(\mu\left[(\nabla \boldsymbol{u})^T - \frac{2}{3} tr\,(\nabla \boldsymbol{u})^T \boldsymbol{I}\right]\right) = -\nabla p + \rho \boldsymbol{f} \tag{3}$$

where $\boldsymbol{f}$ is body force vector, p is the pressure, μ denotes the dynamic viscosity of the cooling fluid [42]. In (3), the operator tr takes the trace of a tensor in 3-dimensions. The exchange of energy is modeled in both domains; in the fluid as

$$\frac{\partial (\rho h)}{\partial t} + \nabla \cdot (\rho \boldsymbol{u} h) + \frac{\partial (\rho k)}{\partial t} + \nabla \cdot (\rho \boldsymbol{u} k) - \frac{\partial p}{\partial t} = \rho \boldsymbol{u} \cdot \boldsymbol{g} + \nabla \cdot \left(\alpha_{eff} \nabla h\right) + \rho r + \rho \mathrm{MRF} \tag{4}$$

where h is the enthalpy of the coolant [43], [44]. Enthalpy is sum of internal energy of the fluid system and its work on its boundaries. The term r is representing the source terms from radiation heat transfer, multiple reference frame (MRF) is another source term dependent on type of solutions. k is the kinetic energy of the cooling fluid. The term α_{eff} is the sum of laminar and turbulent thermal diffusivities. Thermal diffusivity α is $\frac{\kappa}{C_P}$ and κ is the thermal conductivity of the coolant. Finally, energy equation in the solid is modeled as

$$\frac{\partial (\rho C_P T)}{\partial t} - \nabla(\kappa \nabla T) = 0 \tag{5}$$

where κ is the thermal conductivity of the different materials used for modelling [41]. For the creation of computational meshes, the hexahedral volume mesher from OpenFOAM is used. Both the meshing and computations are parallelized on min. 64 CPUs.

D. DISCIPLINE STRUCTURAL MECHANICS

FEM in 3D is used to quantify thermomechanical loads on critical parts of the battery module. In this approach, the cell tabs are taken as hot spots and the dissipation from one hotspot region to another region through a soldered tab is modeled. The software tool used for the purpose is Calculix [45] which quantifies the strain using the Lagrangian strain tensor E for elastic media. For deformation plasticity, the Eulerian strain tensor e and the deviatoric elastic left Cauchy-Green tensor is

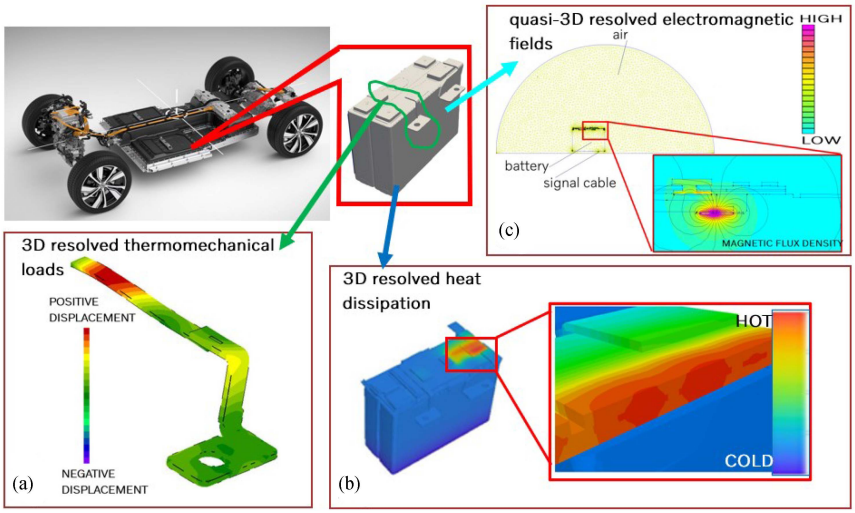

FIGURE 11. The vehicle as a system level modelling instance. In the inset (a) 3D FEM model for thermal elongation for the battery busbar (b) 3D FEM model for conjugate heat transfer analysis for the battery module hot spot distribution (c) quasi-3D FEM model for magnetostatics.

used for incremental plasticity [46]. In the Cartesian coordinate system, the Lagrangian strain satisfies:

$$E_{KL} = (U_{K,L} + U_{L,K} + U_{M,K}U_{M,L})/2, \quad K, L, M = 1, 2, 3 \tag{6}$$

where U_K are the displacement components in the material frame of reference and repeated indices imply summation over the appropriate range. In a linear analysis, this reduces to the following form [46]:

$$E_{KL} = (U_{K,L} + U_{L,K})/2, \quad K, L = 1, 2, 3 \tag{7}$$

The Eulerian strain will satisfy:

$$e_{kl} = (u_{k,l} + u_{l,k} - u_{m,k}u_{m,l})/2, \quad k, l, m = 1, 2, 3 \tag{8}$$

where u_k are the displacements components in the spatial frame of reference. The deviatoric elastic left Cauchy-Green tensor is defined by [46]:

$$\bar{b}^e_{kl} = J^{e-2/3} x^e_{k,K} x^e_{l,K} \tag{9}$$

where J^e is the elastic Jacobian and $x^e_{k,K}$ is the elastic deformation gradient. The stress measure consistent with the Lagrangian strain is the second Piola-Kirchhoff stress S. This stress is for all applications, can be transformed into the first Piola-Kirchhoff stress P and into the Cauchy stress t. All input and output to the used FEM tool is in terms of true stress [46].

E. DISCIPLINE ELECTROMAGNETICS

To cover eventual crosstalk in tightly packaged vehicle platforms, EMI is quantified using a magnetostatic approach. Here a switching effect in the battery electronics is affecting a signal cable in the vicinity. In Fig. 11 battery module is shown in quasi-3D domain, where symmetry conditions represent the direction into the page. The magnetic flux created is shown in enlarged inset. Incorporating solenoidal property of magnetic flux, Ampère's circuit law and non-linear constitutive relationship for materials [47], a FEM based tool [48] solves the EMI problem via time-stepping. FEM calculations start from the given current condition on the battery management system electronics, which

$$\nabla \times \left(\frac{1}{\mu(\overrightarrow{B})} \nabla \times \overrightarrow{A} \right) = \overrightarrow{J} \tag{10}$$

will give $\overrightarrow{A}$, afterwards curl of $\overrightarrow{A}$

$$\nabla \times \overrightarrow{A} = \overrightarrow{B} \tag{11}$$

Solving (11) will provide a magnetic flux density distribution on an arbitrary battery section with prescribed material information, an example of which is shown in Fig. 11. The inductance couples the magnetic flux linkage to the current producing the flux linkage. In this work the current induced in a conductor will be quantified using FEM.

$$L = \frac{\lambda}{i} \tag{12}$$

where L is induction, λ is flux linkage by the current i.

F. MACHINE LEARNING

1) PATTERN RECOGNITION FOR CHARGING POWER TRANSIENTS

PCA uses an orthogonal transformation to project the original data onto new components that better describe the data, that have been created through linear combination of the original features. For finding the principal components, PCA uses a method called Singular Value Decomposition (SVD), which has the following equation [30]:

$$M = U \Sigma V^T \tag{13}$$

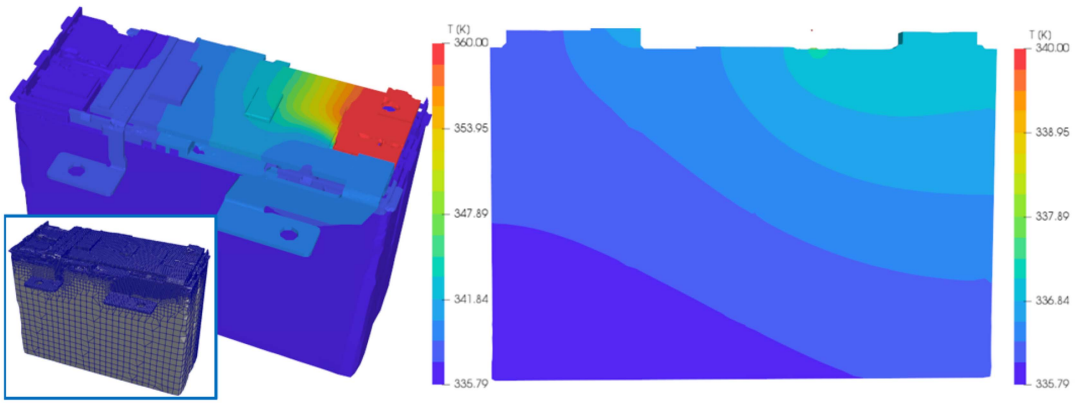

FIGURE 12. 3D FEM model for conjugate heat transfer analysis. Perspective view with temperature field with an inset showing mesh detail on the left and XY-section temperature distribution plot on the righthand side.

SVD diagonalizes any real or complex matrix, e.g. a matrix of charging power transient spline control points as columns and individual charging power transient concept as rows. The output of SVD is three matrices: U, with the left-singular vectors of the input matrix as columns; Σ, a diagonal matrix with the singular values of the input matrix on the diagonal; and transpose of V, with the right-singular vectors of the input matrix as rows. The right-singular vectors are the principal components and the singular values describe how important each component is.

2) PATTERN RECOGNITION FOR CUSTOMER BEHAVIOR

A clustering algorithm is used to cluster the customer behavior. In this the assumption is that the customers who use the most energy will need to charge the most. The K-means algorithm divides a set of N samples X into K separate clusters C, each described by the mean μ_j of the samples in the cluster.

$$\sum_{i=0}^{n} \min(||x_i - \mu_j||^2) \tag{14}$$

with $\mu_j \in C$. The means are commonly called the cluster centroids. The K-means algorithm aims to choose centroids that minimize the inertia, or within-cluster sum-of-squares criterion [30]. Alternatively, Density Based Scanning (DBSCAN) searches for dense regions of sample probability distribution space for clusters. An improvement of this, the Hierarchical DBSCAN includes the clusters with different magnitude of density [49]. In density based clustering, excess of mass of C is described for an arbitrary density function f and C spans a subset of f as $C_\lambda = \{x \in C | f(x) \geq \lambda\}$ as formulated in 15 [49].

$$E(C,\ \lambda) = \int_{C_\lambda} (f(x) - \lambda) dx, \tag{15}$$

where λ is representing the level for density clusters.

VI. RESULTS

A. RESULTS FROM SYSTEM-OF-SYSTEM LEVEL MODELLING

For the MOGA with the chosen cross-over rate, the result of the breeding process is a population comprised of the 60 best parent design points (aka. the elitist strategy) plus 100 new child design points. The EA optimization process will be terminated after either certain number of iterations (generations of the EA) or a finite number of function evaluations. Total number of concept candidates for the study is about 200.

B. RESULTS FROM FEM IN DISCIPLINE HEAT TRANSFER

The MOGA based agent receives the dissipated heat from the loss computations from the Thévenin-circuit model of the battery module to communicate this as a heat source to 3D FEM computations. In this model, the high detail of the geometry and material physics are retained through a mesh size of ca. 556000. In an effort to capture all the physics, FEM model comprises 37 individual regions with individual thermophysical parameters and individual mesh. The Finite Volume Method mesh is hexa-dominant. In Fig. 12 a representative computation results for discipline heat transfer is shown. The operation of the battery leads to heat release, which in turn will be distributed throughout the 37 matching mesh regions creating the battery model.

C. RESULTS FROM FEM IN DISCIPLINE STRUCTURAL MECHANICS

3D FEM is used to quantify strain due to heating of two different metal regions in perfect contact to each other. A tetrahedra dominant mesh of size ca. 2700 elements is prepared as shown in Fig. 13. For discipline structural mechanics, the MOGA agent receives the dissipated heat from the loss computation from the Thévenin-circuit model of the battery module to propagate this further as a temperature front to 3D FEM based structural mechanics computations. As detailed in [50], the lumped parameter models may lack the accurate geometric detail, which may include intrigue geometric detail and material anisotropy. When ML is applied to reduced order models, the learned variance may be due to the lacking features lumped as agglomerate detail. The high detail of the geometry and material physics are retained in the structural mechanics model for good accuracy in 3D.

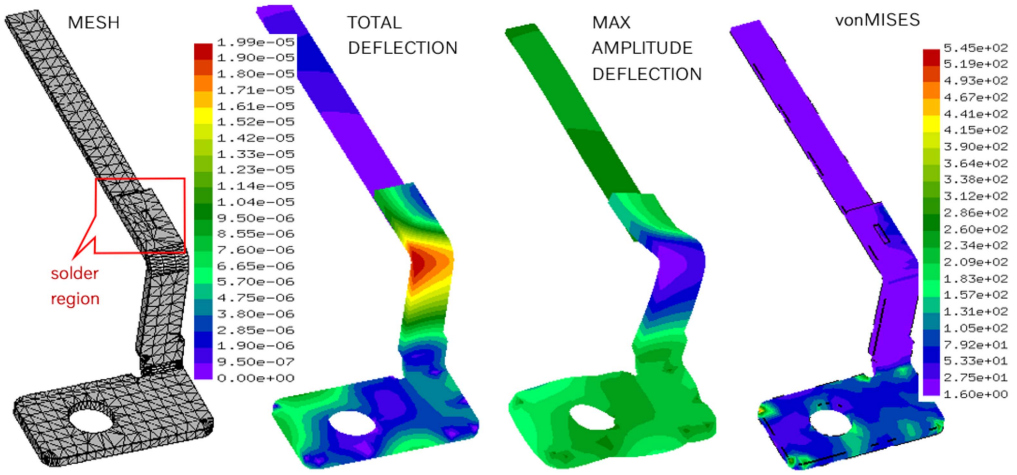

FIGURE 13. Example results by 3D FEM model for thermal elongation of the battery tab.

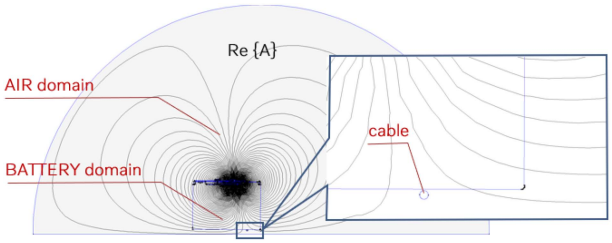

FIGURE 14. The quasi-3D FEM model for magnetostatics. Cable position detailed in the inset. Real part of the magnetic field potential is depicted as field lines. For this field, maximum magnetic field flux reaches to 1.4E-4 T.

D. RESULTS FROM FEM IN DISCIPLINE ELECTROMAGNETICS

A quasi-3D FEM method, where the third direction is modeled as symmetry conditions, is used to compute the electromagnetic behavior. For this, a representative switching effect is assumed in a magnetic material in the vicinity of the battery cell using through a mesh size of ca. 34000. A nearby signal cable is represented with a copper wire just below the battery cell illustrated in Fig. 14. Accordingly, each time a new charging power transient is designed by the MOGA agent, a different magnetic flux will be created by the battery control electronics. This magnetic flux will be radiated to the victim represented by the copper wire under the battery and a voltage will be induced. The MOGA agent is designed to minimize this voltage. In the inset, the detail in the cable vicinity is depicted. Magnetic field potential lines in the XY-plane shows the region in Fig. 14 where the cable is protected from the dipole due to the switching by being positioned in a silent region of the magnetic field.

E. PATTERN RECOGNITION FOR REPRESENTATIVE CHARGING POWER TRANSIENTS

In this study, PCA is used to represent principal types of charging power transients with the battery chemistry at hand. The 8 principal components of all the populated charging power transients are listed in the Table 1. It can be observed

TABLE 1. 8 Principal Components in Charging Power Transients

Charging Power Transients	variance	cumsum
Power transient 1	0.145	0.145
Power transient 2	0.122	0.267
Power transient 3	0.098	0.365
Power transient 4	0.092	0.457
Power transient 5	0.080	0.537
Power transient 6	0.076	0.613
Power transient 7	0.067	0.679
Power transient 8	0.058	0.737

that, 7 PCA components contain about 70% of all the information entailed in all the populated charging power transients.

F. PATTERN RECOGNITION FOR REPRESENTATIVE CUSTOMER BEHAVIOR

To represent the customer behavior, a subsampled dataset for 50 drivers from [31] on the speed limit breach - acceleration feature plane is investigated in Fig. 16. On the lefthand side of Fig. 16, an HDBSCAN on the speed limit breach - acceleration feature plane discerns seven clusters. Following this step, a K-means clustering algorithm [30] is prescribed to distribute individual driving styles of 50 drivers into seven clusters as shown in the same figure. Thus, a correlation between customer habits and preferences with hard coded performance characteristics of an engineering system like xEV is established. The connection to the driver behavior is addressed via 7 customer clusters representing 7 driving styles. Studying the identified patterns in Fig. 16, there are drivers which are positioned at lower speeds than the actual speed limit who are also decelerating excessively, shown in region in light blue. For charging curve choice, these individuals will receive tailored curves which will include less overall energy as they are recuperating often. On the other side of the Fig. 16, there are drivers who are above the actual speed limits often and accelerate frequently, this driver cluster represented by grey color will receive the charging power transient with the highest energy content.

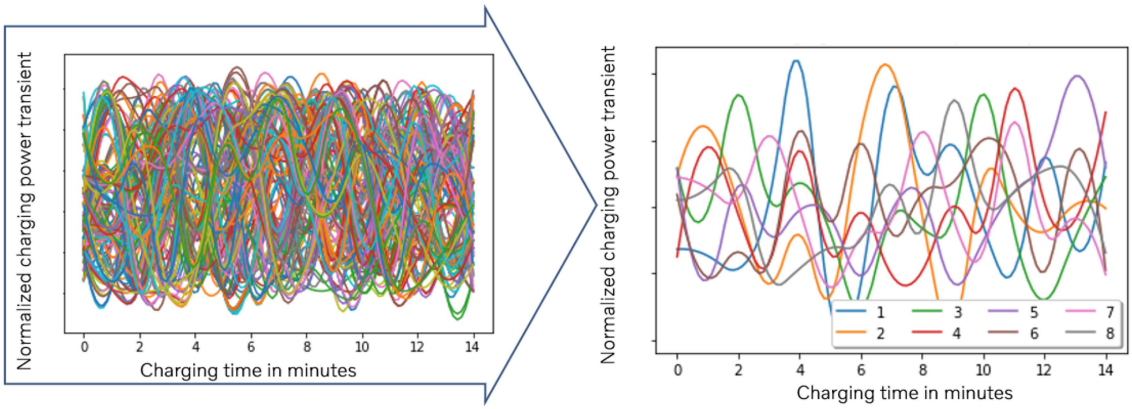

FIGURE 15. Charging power transients reduced via PCA. Eight components capture 74% of charging power transients.

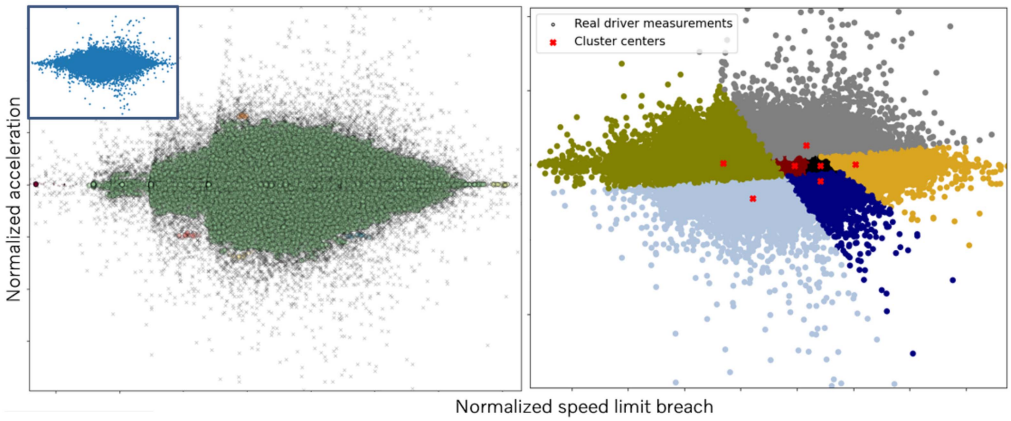

FIGURE 16. Hierarchical DBSCAN and K-means for 50 drivers on the speed limit breach - acceleration feature plane. The original data is shown in left-hand inset.

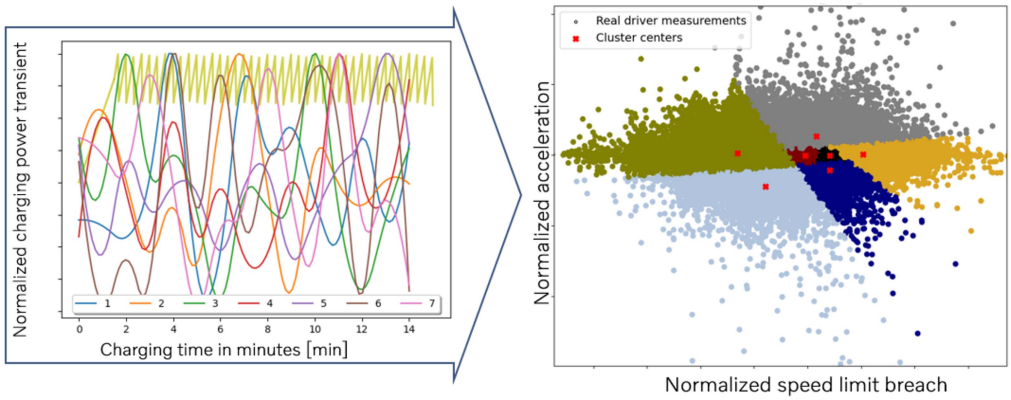

FIGURE 17. Charging curves matched to different driving styles of human automobilists. The pulsed charging limits for a representative charging process is shown in left inset in yellow.

Aligned with the above explained logic, 7 designs for charging power transients are then coupled to 7 principal driving styles as depicted in Fig. 17. It is worth noting that the size of the dataset has an impact on distance based clustering algorithms like K-means. In Fig. 16 with 50 drivers, the seven drivers are distributed principally on the speed limit breach principal component, alternatively, in Fig. 8 with 8 drivers, the drivestyles are distributed on both axes, albeit more dominantly on the speed limit breach direction.

VII. DISCUSSION

Except the system-of-system level and 3D meshing all the physical modeling is done using open-source software. This aligns with UN Secretary-General's Roadmap for Digital Cooperation.

The recourse to use synthetically generated fast charging data is due to the fact that there is no publicly available fast charging data. The method provides a viable approach to populate realistic user data, conform with General Data Protection Regulation.

VIII. CONCLUSION

An RS based approach to devise tailored power transients for xEV charging is presented. The cold-start problem, a known shortcoming for collaborative-filtering based RS, is tackled using a physics-informed approach. Two AI agents are designed to cooperate. A MOGA agent, mimics humans charging maximum electric energy in given time and an RS agent gathering information from charging power transients populated based on battery physics to recommend tailored charging for human drivers. MOGA agent governs detailed multi-physics comprising 3D FEM solutions for thermal, mechanical and electromagnetic disciplines are prescribed to accurately model the heat generation of the battery while filtering the charging power transients incorporating maximum allowable cell temperatures. Introducing clustering and data reduction, the physics of the battery during charging is coupled to the customer choices via the driving dynamics. From hundreds of charging power transients created based on physical models, 7 principle charging power transients are computed. To enable RS cold-start, driving data from an experimental data set is used. Using clustering, 7 principal driving styles from a driving-dynamics point of view were additionally discerned. By combining these two patterns, 50 drivers are matched with 7 power transient curves for xEV fast charging, where there assumed to be no information on charging power transients preferred by the customers were available. The RS based approach will thus be informed by the inherent physics to enable a cold-start ability. The presented solution can easily be extended to contain more customer data as well as dynamic pricing for the electricity.

REFERENCES

[1] United Nations, "United Nations document on sustainable development goals," Accessed: Dec. 25, 2019. [Online]. Available: https://www.un.org/

[2] C. A. Gomez-Uribe and N. Hunt, "The Netflix recommender system: Algorithms, business value, and innovation," *ACM Trans. Manage. Inf. Syst.*, vol. 60, no. 4, Dec. 2016, Art. no. 13.

[3] Q. Ouyang, G. Xu, H. Fang, and Z. Wang, "Fast charging control for battery packs with combined optimization of charger and equalizers," *IEEE Trans. Ind. Electron.*, vol. 680, no. 11, pp. 11076–11086, Nov. 2021.

[4] C. Ji et al., "A personalized fast-charging navigation strategy based on mutual effect of dynamic queuing," *IEEE Trans. Ind. Appl.*, vol. 560, no. 5, pp. 5729–5740, Sep./Oct. 2020.

[5] V. M. Iyer, S. Gulur, S. Gohil, and S. Bhattacharya, "An approach towards extreme fast charging station power delivery for electric vehicles with partial power processing," *IEEE Trans. Ind. Electron.*, vol. 670, no. 10, pp. 8076–8087, Oct. 2020.

[6] H. Tu, H. Feng, S. Srdic, and S. Lukic, "Extreme fast charging of electric vehicles: A technology overview," *IEEE Trans. Transport. Electrific.*, vol. 50, no. 4, pp. 861–878, Dec. 2019, doi: 10.1109/TTE.2019.2958709.

[7] Z. Wang et al., "Overcharge-to-thermal-runaway behavior and safety assessment of commercial lithium-ion cells with different cathode materials: A comparison study," *J. Energy Chem.*, vol. 55, pp. 484–498, 2021.

[8] S. Park, G.-W. You, and D.-J. Oh, "Data-driven state-of-health estimation of EV batteries using fatigue features," in *2016 IEEE Int. Conf. Consum. Electron.*, 2016, pp. 101–102.

[9] R. Soares, N. Djekanovic, O. Wallmark, and P. C. Loh, "Integration of magnified alternating current in battery fast chargers based on DC–DC converters using transformerless resonant filter design," *IEEE Trans. Transp. Electrific.*, vol. 50, no. 4, pp. 925–933, Dec. 2019.

[10] Z. Guo, J. Xu, Z. Xu, M. Mubashir, H. Wang, and X. Mei, "A three-heat-source electro-thermal coupled model for fast estimation of the temperature distribution of a lithium-ion battery cell," *IEEE Trans. Transp. Electrific.*, vol. 80, no. 1, pp. 288–297, Mar. 2022.

[11] X.-G. Yang et al., "Asymmetric temperature modulation for extreme fast charging of lithium-ion batteries," *Joule*, vol. 30, no. 12, pp. 3002–3019, 2019.

[12] O. Aiello, P. S. Crovetti, and F. Fiori, "Susceptibility to EMI of a battery management system IC for electric vehicles," in *2015 IEEE Int. Symp. Electromagn. Compat.*, 2015, pp. 749–754.

[13] Y. Qu, W. Shu, L. Qiu, Y.-C. Kuan, S.-H. Wood Chiang, and J. S. Chang, "A low-profile high-efficiency fast battery charger with unifiable constant-current and constant-voltage regulation," *IEEE Trans. Circuits Syst. I: Reg. Papers*, vol. 670, no. 11, pp. 4099–4109, Nov. 2020.

[14] K. K. Duru, C. Karra, P. Venkatachalam, S. A. Betha, A. A. Madhavan, and S. Kalluri, "Critical insights into fast charging techniques for lithium-ion batteries in electric vehicles," *IEEE Trans. Device Mater. Rel.*, vol. 210, no. 1, pp. 137–152, Mar. 2021.

[15] A. Abd El Baset Abd El Halim, E. Bayoumi, W. El-Khattam, and A. Ibrahim, "Effect of fast charging on lithium-ion batteries: A review," *SAE Int. J. Electrified Veh.*, vol. 120, no. 3, pp. 361–388, Apr. 2023.

[16] S. M. Al-Ghuribi and S. A. Noah, "Multi-criteria review-based recommender system–the state of the art," *IEEE Access*, vol. 7, pp. 169446–169468, 2019.

[17] Z. Teimoori, A. Yassine, and M. S. Hossain, "A secure cloudlet-based charging station recommendation for electric vehicles empowered by federated learning," *IEEE Trans. Ind. Inform.*, vol. 18, no. 9, pp. 6464–6473, Sep. 2022.

[18] Z. Tan, L. Liu, J. Wu, and Y. Zhou, "A charging station recommendation method based on link prediction for cruising electric taxis," in *2022 IEEE 25th Int. Conf. Comput. Supported Cooperative Work Des.*, 2022, pp. 127–132.

[19] Y. Wang, H. T. Luan, Z. Su, N. Zhang, and A. Benslimane, "A secure and efficient wireless charging scheme for electric vehicles in vehicular energy networks," *IEEE Trans. Veh. Technol.*, vol. 71, no. 2, pp. 1491–1508, Feb. 2022.

[20] F. Teng, Z. Ding, Z. Hu, and P. Sarikprueck, "Technical review on advanced approaches for electric vehicle charging demand management, Part I: Applications in electric power market and renewable energy integration," *IEEE Trans. Ind. Appl.*, vol. 560, no. 5, pp. 5684–5694, Sep./Oct. 2020.

[21] S. Deb, M. Pihlatie, and M. Al-Saadi, "Smart charging: A comprehensive review," *IEEE Access*, vol. 10, pp. 134690–134703, 2022.

[22] T. Wei et al., "Fast adaptation for cold-start collaborative filtering with meta-learning," in *2020 IEEE Int. Conf. Data Mining*, 2020, pp. 661–670.

[23] M. Rouhani, A. D. Sappa, and E. Boyer, "Implicit B-spline surface reconstruction," *IEEE Trans. Image Process.*, vol. 240, no. 1, pp. 22–32, Jan. 2015.

[24] Z. Deng, L. Xu, H. Liu, X. Hu, Z. Duan, and Y. Xu, "Prognostics of battery capacity based on charging data and data-driven methods for on-road vehicles," *Appl. Energy*, vol. 339, 2023, Art. no. 120954.

[25] Y. Wang et al., "Data-driven capacity estimation of commercial lithium-ion batteries from voltage relaxation," *Nature Commun.*, vol. 13, 2022, Art. no. 2261.

[26] "Battery data," CALCE, James Clark School of Engineering, Univ. Maryland, College Park, MD,USA, Accessed: Aug. 14, 2024. [Online]. Available: https://calce.umd.edu/battery-data

[27] B. Saha and K. Goebel, "Battery data set," NASA Prognostics Data Repository, NASA Ames Res. Center, Moffett Field, CA, USA, 2007. Accessed: Aug. 14, 2024. [Online]. Available: https://www.nasa.gov/intelligent-systems-division/discovery-and-systems-health/pcoe/pcoe-data-set-repository/

[28] ViBilaegare (in Swedish), "Test: Ford mustang Mach-e, Polestar 2, Skoda Enyaq, Volkswagen ID 4 Och Volvo xc40, 2021," Internet version, Accessed: Aug. 09, 2024. [Online]. Available: https://www.vibilagare.se/test/biltester/nybilstest/test-ford-mustang-mach-e-polestar-2-skoda-enyaq-volkswagen-id-4-och-volvo
[29] L. Michael Waskom, "Seaborn: Statistical data visualization," *J. Open Source Softw.*, vol. 60, no. 60, 2021, Art. no. 3021.
[30] F. Pedregosa et al., "Scikit-learn: Machine learning in Python," *J. Mach. Learn. Res.*, vol. 12, pp. 2825–2830, 2011.
[31] S. Karlsson, "The Swedish car movement data project," 2013. Accessed: Jan. 25, 2022. [Online]. Available: http://publications.lib.chalmers.se/records/fulltext/187380/local_187380.pdf
[32] W. Li, Y. Zhao, X. Chen, Y. Xiao, and Y. Qin, "Detecting alzheimer's disease on small dataset: A knowledge transfer perspective," *IEEE J. Biomed. Health Informat.*, vol. 230, no. 3, pp. 1234–1242, May 2019.
[33] R. Shao and X.-J. Bi, "Transformers meet small datasets," *IEEE Access*, vol. 10, pp. 118454–118464, 2022.
[34] J. A. Prenner and R. Robbes, "Making the most of small software engineering datasets with modern machine learning," *IEEE Trans. Softw. Eng.*, vol. 480, no. 12, pp. 5050–5067, Dec. 2022.
[35] L. Brigato, B. Barz, L. Iocchi, and J. Denzler, "Image classification with small datasets: Overview and benchmark," *IEEE Access*, vol. 10, pp. 49233–49250, 2022.
[36] B. M. Adams et al., "A multilevel parallel object-oriented framework for design optimization, parameter estimation, uncertainty quantification, and sensitivity analysis: Version 5.1 User's Manual," Sandia Tech. Rep. SAND2010-2183, 2010.
[37] L. Buffoni et al., "Open source languages and methods for cyber-physical system development: Overview and case studies," *Electronics*, vol. 100, no. 8, 2021, Art. no. 902.
[38] D. Bernardi, E. Pawlikowski, and J. Newman, "A general energy balance for battery systems," *J. Electrochem. Soc.*, vol. 132, no. 1, Jan. 1985, Art. no. 5.
[39] X. Hu, W. Liu, X. Lin, and Y. Xie, "A comparative study of control-oriented thermal models for cylindrical li-ion batteries," *IEEE Trans. Transp. Electrific.*, vol. 50, no. 4, pp. 1237–1253, Dec. 2019.
[40] W. Versteeg and H. K. Malalasekera, *An Introduction to Computational Fluid Dynamics*. London, U.K.: Pearson Educ. Ltd., 2007.
[41] "OpenFOAM," Accessed: Jan. 13, 2020, [Online]. Available: https://openfoam.org/
[42] Y. Li, "Implementation of multiple time steps for the multi-physics solver based on chtmultiregionfoam," in *Proc. CFD OpenSource Softw.*, H. Nilsson, Ed., 2016, pp. 20–22.
[43] "Energy equation in OpenFOAM," Accessed: Jan. 25, 2020. [Online]. Available: https://cfd.direct/openfoam/energy-equation/
[44] "Chtmultiregionfoam-solver for steady or transient fluid flow and solid heat conduction," Accessed: Jan. 25, 2020. [Online]. Available: https://openfoamwiki.net/index.php/ChtMultiRegionFoam
[45] "Calculix software," Accessed: Jan. 25, 2022. [Online]. Available: https://www.calculix.de
[46] MIT, "Calculix theory," Accessed: Jan. 25, 2022. [Online]. Available: https://web.mit.edu/calculix_v2.7/CalculiX/ccx_2.7/doc/ccx/node23.html
[47] D. K. Cheng, *Field and Wave Electromagnetics*. Reading, MA, USA: Addison-Wesley, 1989.
[48] D. C. Meeker, "Finite element method magnetics, version 4.2," Accessed: Jan. 11, 2021. [Online]. Available: https://www.femm.info
[49] L. McInnes and J. Healy, "Accelerated hierarchical density based clustering," in *2017 IEEE Int. Conf. Data Mining Workshops*, 2017, pp. 33–42.
[50] S. Amirpour et al., "Highly thermal conductive graphene-based Heatsink tailored for electric propulsion SIC-based inverter," *Appl. Thermal Eng.*, vol. 243, 2024, Art. no. 122548.

RAIK ORBAY received the B.Sc. and M.Sc. degrees in aeronautical engineering from ITU, Istanbul, Türkiye, the DEA in energy engineering from SUPAERO, Toulouse, France, and the Ph.D. degree in mechanical engineering from LTH, Lund, Sweden. He is currently the Technical Expert with Advanced Simulation Methods, Volvo Car Corporation - Propulsion and Energy, Gothenburg, Sweden and as a Researcher with the Department of Electrical Engineering, Chalmers University of Technology, Gothenburg, Sweden. His research interests include experimental / FEM based synthetic data and automation for sustainable engineering.

ADITYA PRATAP SINGH received the bachelor's degree (*with cum laude*) in mechanical and automation engineering, and the M.Sc. degree in vehicle engineering from the KTH Royal Institute of Technology, Stockholm, Sweden, in 2021. Since 2021, he has been with Volvo Car Corporation, as a CAE Engineer and a part of Battery Component and Propulsion System Level Modelling Team. He has supervised four master thesis projects related to electric propulsion controls and electric machine design. He was also a Powertrain Development Engineer with FEV in India and Malaysia. He has authored and coauthored 20 research papers. His research interests include advanced research engineering projects focused on converters and battery technology. At Volvo Car Corporation, his work on Vehicle-2-Grid charging controls was among top 3 Volvo Cars Invention of the Year for the year 2024.

JOHANNES EMILSSON received the M.Sc. degree in applied mechanics, structural dynamics from the Chalmers University of Technology, Gothenburg, Sweden, 2010. He is currently a System Simulation Architect with Volvo Car Corporation - Vehicle Testing and Integration, Gothenburg. His research interests include CAE modeling, simulation automation, multiphysics optimization, and system design.

MICHELE BECCIANI received the Ph.D. degree in energy engineering. He is currently a Feature Architect with the Volvo Group, specializing in the development of future transportation powertrains. His research interests include optimizing electric vehicle propulsion systems, particularly in energy management and cooling techniques for electric motors, multi-objective optimization, thermal management, and sustainable automotive technologies, with a goal to enhance vehicle efficiency and performance.

EVELINA WIKNER (Member, IEEE) received the B.Sc. degree in chemical engineering and engineering physics, the M.Sc. degree in nanoscience and nanotechnology, and the Ph.D. degree in electrical engineering from the Chalmers University of Technology, Gothenburg, Sweden. She is currently an Assistant Professor with the Department of Electrical Engineering, Chalmers University of Technology. Her research interests include Li-ion and Na-ion batteries, optimizing utilization and lifetime in stationary and electromobility applications with a focus on sustainability. Her research interests mainly include testing and modeling of Li-ion and Na-ion batteries, from detailed cell modeling to system aspects.

VICTOR GUSTAFSON received the M.Sc. degree in engineering from Lund's University, Lund, Sweden, in 2015. He is currently a Concept Leader with Volvo Car Corporation - Propulsion and Energy, Gothenburg, Sweden. His research interests include in power electronics, HV & LV- system, propulsion (electrical), charging, power supply and CAE modelling, with an emphasis on future battery electric platform solutions in automotive industry.

TORBJÖRN THIRINGER (Senior Member, IEEE) received the M.Sc. and Ph.D. degrees from the Chalmers University of Technology, Göteborg, Sweden, in 1989 and 1996, respectively. He is currently a Professor of applied power electronics with the Chalmers University of Technology. His research interests include the modeling, control and grid integration of wind energy converters into power grids as well as power electronics and drives for other types of applications, such as electrified vehicles, buildings and industrial applications.